

# Multiple stationary states for deformable drops in linear Stokes flows

J. Bławdziewicz,<sup>1</sup> Vittorio Cristini,<sup>2</sup> and Michael Loewenberg<sup>2</sup>

<sup>1</sup>*Department of Mechanical Engineering, Yale University,  
P.O. Box 20-8286, New Haven, CT 06520, USA*

<sup>2</sup>*Department of Chemical Engineering, Yale University,  
P.O. Box 20-8286, New Haven, CT 06520, USA*

## Abstract

Using a small-deformation expansion and numerical simulations we study stationary shapes of viscous drops in two-dimensional linear Stokes flows with nonzero vorticity. We show that high-viscosity drops in flows with vorticity magnitude  $\beta \ll 1$  have two branches of stable stationary states. One branch corresponds to nearly-spherical drops stabilized primarily by rotation, and the other to elongated drops stabilized primarily by capillary forces. For drop-to-continuous-phase viscosity ratios beyond a critical value  $\lambda_c$ , the rotationally-stabilized solution exists in the absence of capillary stresses, because the rate of drop deformation (but not rotation) decreases with drop viscosity. We show that  $\lambda_c = 10\beta^{-2}$ , and the capillary stresses required for drop stability vanish at  $\lambda_c$  with exponent  $1/2$ , as required by flow-reversal symmetry.

The behavior of viscous drops in creeping flows is relevant to the dynamic properties of fluid-fluid dispersions. Thus, drop dynamics has been extensively studied experimentally [1–4], theoretically [5–7], and by numerical simulations [8–11].

The nonlinear character of drop dynamics in Stokes flow results from the nonlinear dependence of the flow field on the drop shape. Nonlinear effects include the existence of a stable and an unstable branch of stationary shapes [7]. The branches merge and disappear at a critical value of the capillary number (dimensionless flow strength). Despite of the nonlinear character of the system, the possibility of multiple *stable* branches of stationary shapes has not been explored. Here we examine this situation.

We focus on two-dimensional linear incident flows, defined by the velocity gradient

$$\nabla \mathbf{u} = \dot{\gamma} \begin{pmatrix} 0 & 1 + \beta & 0 \\ 1 - \beta & 0 & 0 \\ 0 & 0 & 0 \end{pmatrix}, \quad (1)$$

where  $\beta$  is the vorticity parameter ( $\beta = 0$  corresponds to a two-dimensional strain, and  $\beta = 1$  to shear flow). Drop evolution in such flows depends on  $\beta$ , the capillary number  $C = \mu a \dot{\gamma} / \sigma$  ( $\frac{4}{3}\pi a^3$  is the drop volume, and  $\sigma$  is the interfacial tension), and the viscosity ratio  $\lambda = \hat{\mu} / \mu$  of the drop-phase and continuous-phase fluids.

Stationary shapes of a drop in an incident velocity field (1) may be produced by two stabilizing mechanisms: (i) drop rotation by the vorticity of the external flow, and (ii) drop relaxation due to capillary stresses. Rotation is particularly important for high-viscosity drops, because the time scale for drop rotation  $t_r = (\beta \dot{\gamma})^{-1}$  is independent of  $\lambda$ , unlike the time scales for capillary relaxation  $t_\sigma = \lambda \mu a / \sigma$  and drop convection by the straining component of the flow  $t_d = \lambda \dot{\gamma}^{-1}$ , both of which increase with  $\lambda \gg 1$ .

In this letter, we demonstrate that two branches of stable stationary drop shapes exist for highly-viscous drops in nearly-straining flows with  $0 < \beta \lesssim 0.4$  as a result of stabilizing mechanisms (i) and (ii). The first branch is predominantly stabilized by drop rotation, and the second by capillary relaxation.

To explore the branch structure of stationary drop shapes, we use a small deformation expansion [5]. Accordingly, the position  $r_S$  of the drop interface is expanded in spherical harmonics

$$r_S/a = 1 + \alpha + f, \quad (2)$$

$$f = 2^{1/2} \sum_{l,m} [f'_{lm} \text{Re}(Y_{lm}) + f''_{lm} \text{Im}(Y_{lm})], \quad (3)$$

where  $l > 0$ ,  $l \geq m \geq 0$ , and  $f''_{l0} = 0$ . The isotropic term  $\alpha$  is required for volume conservation. Assuming that drop shapes preserve the symmetry of the flow (1), only even powers of  $l$  and  $m$  contribute to the expansion (3).

For simplicity, we restrict our analysis to the subspace  $l = 2$ . Thus the drop shape  $f$  has three independent components:  $f'_{22}$ ,  $f''_{22}$ , and  $f'_{20}$ , corresponding to deformation along the the  $x$  axis, straining axis  $x = y$ , and the  $z$  axis. In the evolution equations for the drop shape we retain terms up to order  $O(f^2)$ . This description captures the essential features of the system, and for nearly-straining flows yields quantitative asymptotic results. For the incident flow (1), the truncated evolution equations are

$$\dot{f}'_{20} = \lambda^{-1}(d_{11}f''_{22} + d_{12}f'_{20}f''_{22}) - \lambda^{-1}C^{-1}[D_1f'_{20} - D_2(f'^2_{20} - f'^2_{22} - f''^2_{22})] \quad (4a)$$

$$\dot{f}'_{22} = -2\omega f''_{22} + \lambda^{-1}d_{21}f'_{22}f''_{22} - \lambda^{-1}C^{-1}(D_1f'_{22} + 2D_2f'_{20}f'_{22}), \quad (4b)$$

$$\dot{f}''_{22} = 2\omega f'_{22} + \lambda^{-1}(d_{31} + d_{32}f'_{20} + d_{33}f'^2_{20} + d_{34}f'^2_{22} + d_{35}f''^2_{22}) - \lambda^{-1}C^{-1}(D_1f''_{22} + 2D_2f'_{20}f''_{22}), \quad (4c)$$

where the dot denotes differentiation with respect to time normalized by  $\dot{\gamma}^{-1}$ . Terms involving coefficients  $d_{ij}$  correspond to drop deformation by the flow, and terms involving  $D_i$  are associated with capillary relaxation. The coefficients  $d_{ij}$  and  $D_i$  are functions of  $\lambda$ , and have finite limits for  $\lambda \rightarrow \infty$ . The remaining two terms correspond to the rotation of a rigid particle with shape  $f$  by the external flow. The angular velocity of this rotation is

$$\omega = -\beta + c_1 f'_{22}, \quad (5)$$

where  $c_1 = \frac{3}{2}(15/\pi)^{1/2}$  characterizes the rotation produced by the straining component of the flow. Equations (4) and expressions for the coefficients  $d_{ij}$  and  $D_i$  can be obtained by transforming Eq. (2.2) in Ref. [5] into the spherical-harmonics representation (3).

An asymptotic analysis of the bifurcation that produces two branches of stationary drop shapes can be performed for highly-viscous drops in strain-dominated flows. The bifurcation occurs in the regime where the effects of drop deformation by the straining component of the flow, drop rotation, and capillary relaxation are comparable. For high-viscosity drops a balance between drop deformation and rotation corresponds to  $\lambda^{-1} \sim \omega f'_{22}$ , and a balance between relaxation and rotation corresponds to relations  $(\lambda C)^{-1} f'_{22} \sim \omega f''_{22}$  and  $(\lambda C)^{-1} f''_{22} \sim \omega f'_{22}$ . We also assume that near the bifurcation point the two contributions to the angular velocity (5) are of the same order but do not cancel, i.e.,  $\omega \sim \beta \sim f'_{22}$ .

The above assumptions yield scaling relations

$$\lambda^{-1} = \beta^2 \bar{\eta}, \quad C^{-1} = (\beta \bar{\eta})^{-1} \bar{\kappa}, \quad (6a,b)$$

$$f'_{22} = \beta \bar{f}'_{22}, \quad f''_{22} = \beta \bar{f}''_{22}, \quad (6c,d)$$

where  $\bar{\eta}$ ,  $\bar{\kappa}$ , and  $\bar{f}$  are the rescaled viscosity, capillary, and shape parameters. Relation (6a) indicates that for  $\beta \ll 1$ , high drop viscosity is needed to achieve a balance between deforming viscous forces and the rotational and capillary stabilizing mechanisms. Relations (6c,d) show that drop deformation is small in the regime considered; therefore, the small-deformation equations (4) can be used to determine stationary drops shapes close to the bifurcation point in nearly straining flows. Inserting relations (6) into Eq. (4a) yields  $f'_{20} = O(\beta^2)$ ; thus, to the leading order, the shape component  $f'_{20}$  is unimportant.

The asymptotic form of the evolution equations in the regime  $\beta \ll 1$  is obtained by inserting scaling relations (6) into Eqs. (4b) and (4c), and retaining only the leading-order terms. For stationary states we find

$$2(1 - c_1 \bar{f}'_{22}) \bar{\kappa}^{-1} \bar{f}''_{22} - D_1^{(0)} \bar{f}'_{22} = 0, \quad (7a)$$

$$- 2(1 - c_1 \bar{f}'_{22}) \bar{f}'_{22} + \bar{\eta} d_{31}^{(0)} - \bar{\kappa} D_1^{(0)} \bar{f}''_{22} = 0, \quad (7b)$$

where  $D_1^{(0)} = \frac{20}{19}$  and  $d_{31}^{(0)} = \frac{2}{3}(\frac{5}{3}\pi)^{1/2}$  are the high-viscosity limits of the corresponding coefficients in Eqs. (4).

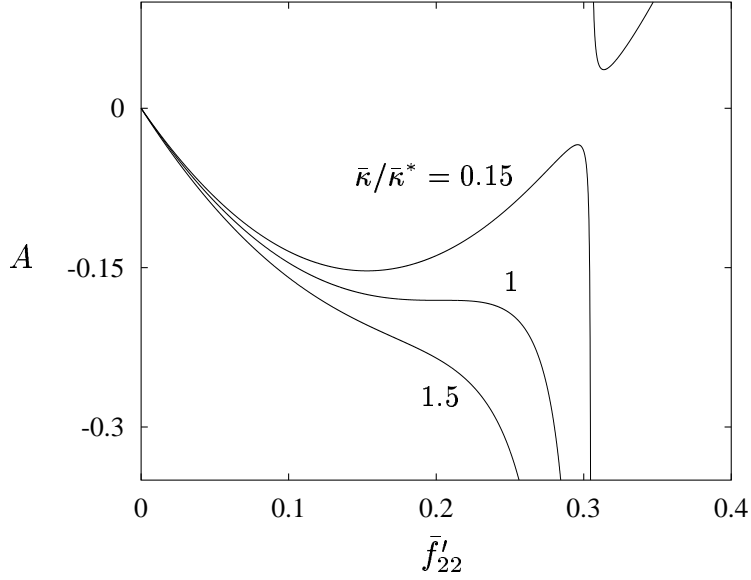


FIG. 1: Function  $A(\bar{f}'_{22})$  for a subcritical, critical, and supercritical value of parameter  $\bar{\kappa}$  (as labeled).

Solving (7a) for  $f''_{22}$  and inserting the result into (7b) yields

$$A(\bar{f}'_{22}) + \bar{\eta}d_{31}^{(0)} = 0, \quad (8)$$

where

$$A(\bar{f}'_{22}) = -2(1 - c_1\bar{f}'_{22})\bar{f}'_{22} - \frac{1}{2}(D_1^{(0)}\bar{\kappa})^2 \frac{\bar{f}'_{22}}{1 - c_1\bar{f}'_{22}}. \quad (9)$$

Since  $\bar{\eta} > 0$ , solutions of Eq. (8) are constrained to the range  $0 < \bar{f}'_{22} < 1/c_1$ , where  $A(\bar{f}'_{22})$  is negative. Each solution  $\bar{f}'_{22}$  corresponds to a single value of  $f''_{22}$  according to Eq. (7a). The typical behavior of  $A(\bar{f}'_{22})$  is shown in Fig. 1 for several values of the rescaled capillary parameter  $\bar{\kappa}$ .

In the regime  $\bar{\kappa} \geq \bar{\kappa}^*$  with

$$\bar{\kappa}^* = \frac{2}{3}\sqrt{\frac{1}{3}/D_1^{(0)}}, \quad (10)$$

the function  $A(\bar{f}'_{22})$  is monotonic thus, Eq. (8) has a unique solution. For  $\bar{\kappa} \leq \bar{\kappa}^*$  the function  $A(\bar{f}'_{22})$  has a minimum at

$$\bar{f}'_{\min} = \frac{1}{6}c_1^{-1} [5 - (g^{1/3} + g^{-1/3})] \quad (11)$$

and a maximum at

$$\bar{f}'_{\max} = \frac{1}{6}c_1^{-1} \{5 - [(-1)^{2/3}g^{1/3} + (-1)^{-2/3}g^{-1/3}]\}, \quad (12)$$

where  $g = 1 - 2\bar{\kappa}_1^2 - 2i\bar{\kappa}_1(1 - \bar{\kappa}_1^2)^{1/2}$ , and  $\bar{\kappa}_1 = \bar{\kappa}/\bar{\kappa}^*$ . Here, the branch cut of  $z^{1/3}$  is taken along the negative real axis and  $(-1)^{1/3} = \frac{1}{2}(1 + i\sqrt{3})$ , which yields real-valued  $\bar{f}'_{\min}$  and

$\bar{f}_{\max}$ . It follows that for  $\bar{\kappa} \leq \bar{\kappa}^*$ , equation (8) has three solutions  $\bar{f}_1 \leq \bar{f}_0 \leq \bar{f}_2$  in the viscosity range

$$\bar{\eta}_1(\bar{\kappa}) \geq \bar{\eta} \geq \bar{\eta}_2(\bar{\kappa}), \quad (13)$$

where

$$\bar{\eta}_1 = -A(\bar{f}_{\min})/d_{31}^{(0)}, \quad \bar{\eta}_2 = -A(\bar{f}_{\max})/d_{31}^{(0)}. \quad (14a,b)$$

For  $\bar{\eta}$  outside of this range, Eq. (8) has a unique solution.

An analysis of the time-dependent form of the rescaled evolution equations (7) indicates that the branches of drop shapes  $\{1\}$  and  $\{2\}$  corresponding to solutions  $\bar{f}_1$  and  $\bar{f}_2$  are stable, and the branch corresponding to  $\bar{f}_0$  is unstable. The pairs of stable and unstable solutions  $(\bar{f}_i, \bar{f}_0)$  with  $i = 1, 2$  merge and disappear at the critical lines  $\bar{\eta} = \bar{\eta}_i(\bar{\kappa})$ , where turning-point bifurcations occur.

Equations (10)–(12) imply that  $\bar{f}_{\min}$  and  $\bar{f}_{\max}$  merge at  $\bar{\kappa} = \bar{\kappa}^*$ ,

$$\bar{f}_{\min}(\bar{\kappa}^*) = \bar{f}_{\max}(\bar{\kappa}^*) = \frac{1}{2}c_1^{-1}, \quad (15)$$

as do the two stable branches of stationary solutions  $\{1\}$  and  $\{2\}$ . The two lines of critical parameters  $\bar{\eta} = \bar{\eta}_i(\bar{\kappa})$  converge (and disappear) at  $\bar{\kappa} = \bar{\kappa}^*$  and  $\bar{\eta} = \bar{\eta}^*$ , where

$$\bar{\eta}^* = \bar{\eta}_i(\bar{\kappa}^*) = \frac{16}{27}(c_1 d_{31}^{(0)})^{-1}, \quad (16)$$

according to Eq. (14a). This behavior indicates that the system undergoes a cusp bifurcation at the critical point  $(\bar{\kappa}^*, \bar{\eta}^*)$ . In unscaled variables, the bifurcation point corresponds to  $C = C^*$  and  $\lambda = \lambda^*$ , where

$$C^* = \frac{32}{57\sqrt{3}}\beta, \quad \lambda^* = \frac{135}{16}\beta^{-2}. \quad (17)$$

An analysis of Eqs. (8)–(9) indicates that drop deformation on branch  $\{1\}$  never exceeds  $O(\beta)$ ; thus, the asymptotic solution  $\bar{f}_1$  is accurate in the regime  $\beta \ll 1$ . For viscosity ratios  $\bar{\eta}$  above the critical value

$$\bar{\eta}_c = \bar{\eta}_1(0) = \frac{1}{2}(c_1 d_{31}^{(0)})^{-1} \quad (18)$$

solution  $\{1\}$  exists for all  $\bar{\kappa} \geq 0$ . This branch of solutions is stabilized predominantly by the  $O(\beta)$  drop rotation for  $\bar{\kappa} \ll 1$ .

In unscaled variables, relation (18) corresponds to the critical viscosity

$$\lambda_c = 10\beta^{-2}. \quad (19)$$

The line of critical capillary numbers  $C = C_1(\lambda)$  associated with the critical line  $\bar{\eta} = \bar{\eta}_1(\bar{\kappa})$  diverges at  $\lambda_c$  as

$$C \sim (\lambda_c - \lambda)^{-1/2}, \quad (20)$$

which is obtained from Eq. (13) by evaluating the position of the minimum  $A(\bar{f}_{\min})$  using a regular perturbation of Eq. (9) in  $\bar{\kappa}^2$ . The order of the singularity (20) is associated with the symmetry of Stokes equations with respect to flow reversal  $\{\mathbf{u}, \sigma\} \rightarrow \{-\mathbf{u}, -\sigma\}$ . This

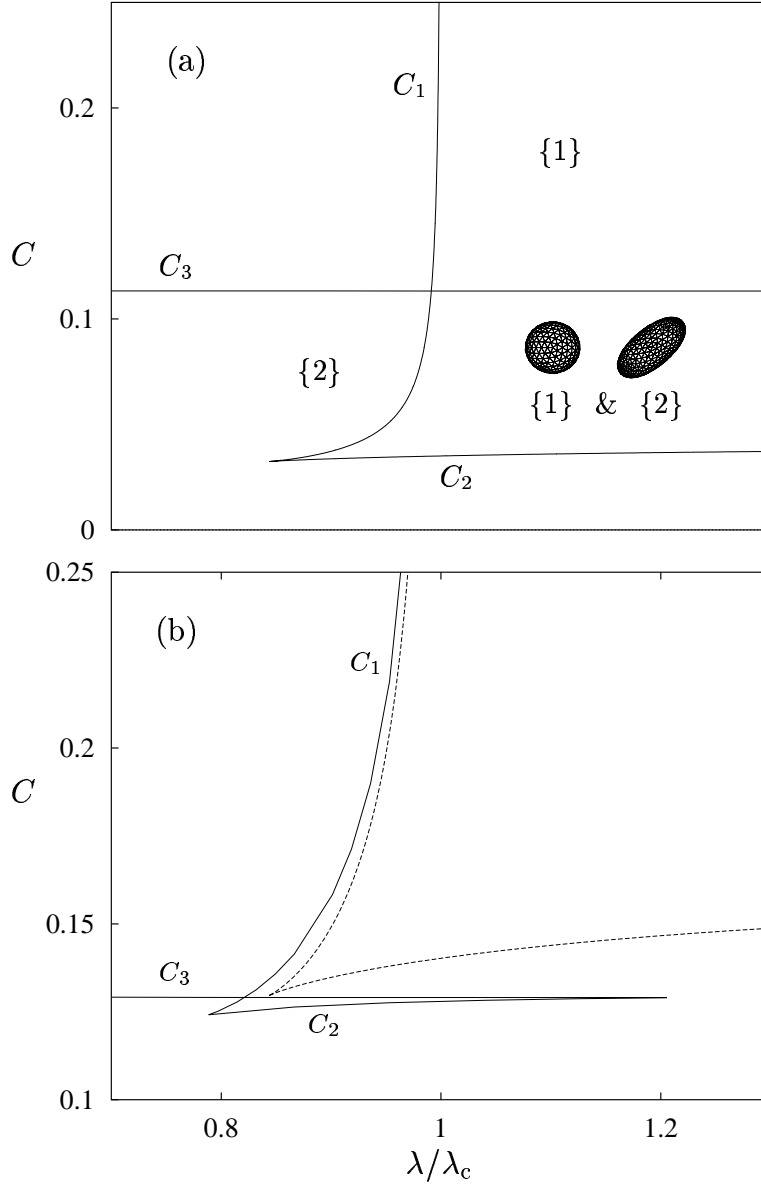


FIG. 2: Boundaries of stability domains for the two branches of stationary drop shapes,  $\beta = 0.1$  (a) and  $\beta = 0.4$  (b). Numerical solution of Eqs. (4) (solid lines), asymptotic formula (14) (dotted lines); numerical and asymptotic results indistinguishable for  $\beta = 0.1$ . Branch  $\{1\}$  exists below and to the right of line  $C_1$ ; branch  $\{2\}$  exists between lines  $C_2$  and  $C_3$ . Stationary drop shapes in coexistence region shown in (a) for  $\lambda/\lambda_c = 0.11$  and  $C \approx C_3$  (results from boundary-integral simulations).

symmetry requires that  $\bar{f}'_{22}$  is an even function and  $\bar{f}''_{22}$  is an odd function of  $\bar{\kappa}$ . As a result  $\bar{f}''_{22} \sim \bar{\kappa}$  for  $\bar{\kappa} \ll 1$ , and  $A(\bar{f}'_{22})$  is a function of  $\bar{\kappa}^2$ . A similar argument applies for finite values of the rotational parameter; thus Eq. (20) is valid for all  $\beta > 0$ .

The singular behavior of the critical line  $C = C_1(\lambda)$  is seen in Fig. 2, where the stability domains of stationary drop shapes  $\{1\}$  and  $\{2\}$  are depicted for two values of the rotational

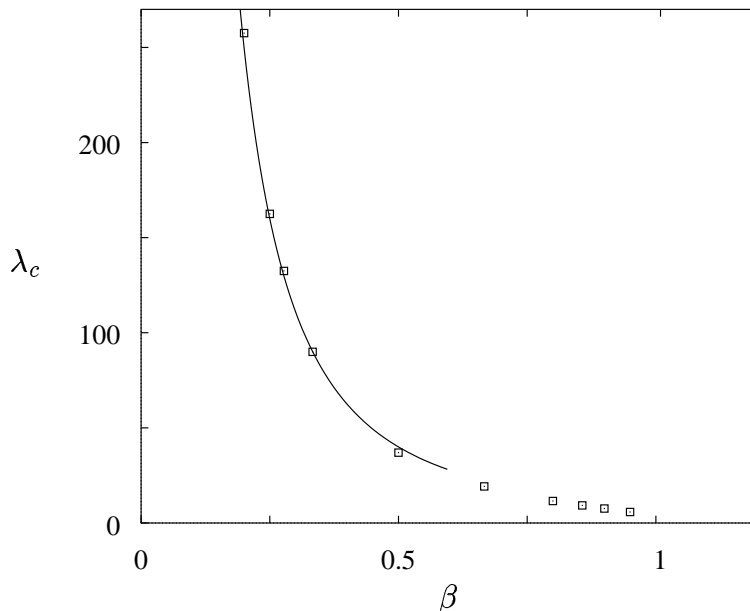


FIG. 3: Critical viscosity as function of rotational parameter. Asymptotic result (19) (solid line); results of boundary-integral simulations (points).

parameter  $\beta$ . The asymptotic result (19) is shown in Fig. 3, along with results from our boundary-integral simulations [11].

In contrast to branch  $\{1\}$  of stationary drop shapes, branch  $\{2\}$  always requires nonzero capillary forces for drop stability. Equation (9) indicates that for small values of  $\bar{\kappa}$ , the maximum of  $A(\bar{f}_{22}')$  is at

$$\bar{f}_{\max} \simeq c_1^{-1} (1 - \frac{1}{2} D_1^{(0)} \bar{\kappa}). \quad (21)$$

Since  $\bar{f}_{\max} \leq \bar{f}_2 \leq c_1^{-1}$ , it follows that

$$\bar{f}_2 \simeq c_1^{-1} \quad \text{for} \quad \bar{\kappa} \ll 1, \quad (22)$$

and thus  $\omega \ll \beta$ , according to Eq. (5). The decrease of the angular velocity  $\omega$ , and the associated loss of the rotational stabilizing mechanism, is accompanied by an increase of drop deformation along the straining axis (cf. Eqs. (7a) and (22)). An analysis of Eq. (9) close to the singular point (22) reveals that the line  $C = C_2(\lambda)$  (corresponding to  $\bar{\eta} = \bar{\eta}_2(\bar{\kappa})$ ) has the asymptotic behavior

$$C_2 = \frac{8}{19} \beta, \quad \lambda \gg \lambda^*. \quad (23)$$

Near this line we obtain  $\bar{f}_{22}'' \simeq c_1^{-1}$ . However,  $\bar{f}_{22}'' \gg 1$  for  $C = O(1)$ , which indicates that the unscaled shape parameter  $f_{22}''$  is  $O(1)$ .

Asymptotic equations (7) are invalid for  $O(1)$  drop deformation, but the behavior of the system in this regime can be qualitatively understood using the unscaled small-deformation equations (4). These equations reveal that an elongated drop in a nearly-straining flow (1) behaves, to the leading-order, as a drop in a purely straining flow. Accordingly, the

stationary branch {2} exists only below a line of critical capillary numbers  $C = C_3(\lambda)$ . A small amount of rotation produces only a slight misalignment the drop with the straining axis. In the regime  $\lambda \gtrsim O(\lambda^*)$  and  $\beta \ll 1$ , small-deformation approximation (4) yields

$$C_3(\lambda) = C_{30} + O(\beta^2), \quad (24)$$

where  $C_{30} = 0.11$ . A boundary-integral solution of the exact evolution equations yields  $C_{30} = 0.101$ .

Equations (23) and (24) indicate that the domain  $C_2 \leq C \leq C_3$  in which the branch of solutions {2} exists, diminishes with increasing  $\beta$ , as illustrated in Fig. 2. This domain disappears entirely for  $\beta$  slightly above the value  $\beta = 0.4$  corresponding to Fig. 2(b).

To summarize, we have shown that there are two branches of stable stationary shapes for drops in two-dimensional Stokes flows (1). On branch {1}, drop deformation is small, and drops are nearly aligned in the  $x$  direction. On branch {2} drop deformation is larger, and drops are approximately aligned with the straining axis.

Branch {1} is primarily stabilized by drop rotation; for viscosity ratios above the critical value (19), this branch exists without the help of capillary stresses. The critical behavior (20) at  $\lambda \approx \lambda_c$  results from flow-reversal symmetry, and thus applies to all two-dimensional linear flows.

It should be possible to experimentally access the two branches of stationary states using a four-roll mill device to produce incident flows (1). The rotationally stabilized stationary state {1} could be obtained by slowly increasing the magnitude of the flow at fixed  $\beta$  (the procedure used in Ref. [3]). The elongated solution {2} could be obtained by quasistatically increasing the rotational component of the flow, starting from pure strain.

The present paper is focused on the domains of drop stability. However, further analysis of the evolution Eqs. (4) indicate that predictions of small-deformation theory for drop dynamics near the critical lines  $C_1, C_2, C_3$  is consistent with the bifurcation mechanism described in our recent study [7].

J.B. was supported by NASA grant No. NAG3-2704; V.C. and M.L. were supported by NASA grant No. NAG3-1935.

- 
- [1] G. I. Taylor, "The formation of emulsions in definable fields of flow," *Proc. R. Soc. Lond. A* **146**, 501–523 (1934).
  - [2] S. Torza, R. G. Cox, and S. G. Mason, "Particle motions in sheared suspensions. 27. Transient and steady deformation and burst of liquid drops," *J. Colloid Interface Sci.* **38**, 395–411 (1972).
  - [3] B. J. Bentley and L. G. Leal, "An experimental investigation of drop deformation and breakup in steady, two-dimensional linear flows," *J. Fluid Mech.* **167**, 241–283 (1986).
  - [4] D. I. Bigio, C. R. Marks, and R. V. Calabrese, "Predicting drop breakup in complex flows from model flow experiments," *Int. Polym. Process* **13**, 192–198 (1998).
  - [5] D. Barthès-Biesel and A. Acrivos, "Deformation and burst of a liquid droplet freely suspended in a linear shear field," *J. Fluid Mech.* **61**, 1–21 (1973).
  - [6] J. M. Rallison, "Note on the time-dependent deformation of a viscous drop which is almost spherical," *J. Fluid Mech.* **98**, 625–633 (1980).
  - [7] J. Bławdziewicz, V. Cristini, and M. Loewenberg, "Critical behavior of drops in linear flows: I. Phenomenological theory for drop dynamics near critical stationary states," *Phys. Fluids* **14**, 2709–2718 (2002).

- [8] M. Tjahjadi, H. A. Stone, and J. M. Ottino, “Satellite and subsatellite formation in capillary breakup,” *J. Fluid Mech.* **243**, 297–317 (1992).
- [9] M. R. Kennedy, C. Pozrikidis, and R. Skalak, “Motion and deformation of liquid drops and the rheology of dilute emulsions in simple shear flow,” *Comput. Fluids* **23**, 251–278 (1994).
- [10] V. Cristini, J. Bławdziewicz, and M. Loewenberg, “Drop breakup in three-dimensional viscous flows,” *Phys. Fluids*. **10**, 1781–1784 (1998).
- [11] V. Cristini, J. Bławdziewicz, and M. Loewenberg, “An adaptive mesh algorithm for evolving surfaces: Simulations of drop breakup and coalescence,” *J. Comput. Phys.* **168**, 445–463 (2001).